

Evidence of filamentary switching and relaxation mechanisms in $\text{Ge}_x\text{Se}_{1-x}$ OTS selectors

Z. Chai⁽¹⁾, W. Zhang^{(1)*}(w.zhang@ljmu.ac.uk), R. Degraeve⁽²⁾, S. Clima⁽²⁾, F. Hatem⁽¹⁾, J. F. Zhang⁽¹⁾, P. Freitas⁽¹⁾, J. Marsland⁽¹⁾, A. Fantini⁽²⁾, D. Garbin⁽²⁾, L. Goux⁽²⁾, G. S. Kar⁽²⁾

⁽¹⁾ Dept. of Electronics & Electr. Eng., Liverpool John Moores University, Liverpool L3 3AF, UK ⁽²⁾ IMEC, Leuven B3001, Belgium

Abstract: Comprehensive experimental and simulation evidence of the filamentary-type switching and V_{th} relaxation mechanism associated with defect charging/discharging in $\text{Ge}_x\text{Se}_{1-x}$ -ovonic threshold switching (OTS) selector is reported. For the first time, area independence of conduction current at both on/off states, Weibull distribution of time-to-switch-on/off ($t_{on/off}$), V_{th} relaxation and its dependence on time, bias and temperature, which is in good agreement with our first-principles simulations in density functional theory, provide strong support for filament modulation by defect delocalization/localization that is responsible for volatile switching.

Introduction: Selector device is critical to suppress the sneak path in high-density cross-point resistive switching memory arrays (Fig. 1a&b). $\text{Ge}_x\text{Se}_{1-x}$ OTS selectors have achieved high on-state current, high half-bias nonlinearity and excellent endurance [1-3]. Theoretical modelling [2] also suggests that the applied electric field modulates the electronic structure of the mis-coordinated Ge-Ge bonds in the amorphous state, appearing as gap/tail states localized/delocalized in space, with signatures of simultaneous carrier hopping and filament crystallization. Despite the progress, electrical experimental evidence supported by theoretical simulation is still lacking. In this paper, based on novel characterization, supported by first-principles simulations, for the first time, we observed: (i) Area-independent conduction current at both on/off states, confirming the modulation of one dominant conduction filament. (ii) Weibull distribution of t_{on}/t_{off} , supporting a random percolation path formed by the first fire (FF) and modulated by switching; (iii) V_{th} relaxation and its dependence on time, bias and temperatures, in agreement with defect delocalization and localization as the dominant volatile switching process.

Device and Characterization: Amorphous $\text{Ge}_x\text{Se}_{1-x}$ films are prepared by room temperature physical vapor deposition (PVD). TiN/GeSe/TiN selector devices were integrated in a 300nm process flow, using a pillar (TiN) bottom electrode which defines the device size down to 50 nm (Fig. 2a). A $\text{Ge}_x\text{Se}_{1-x}$ chalcogenide films control from 20 nm down to 5nm thickness was achieved and passivated with a low-temperature BEOL process scheme. Four different waveforms have been developed in this work: (1) A triangle pulse to record I-V during switching (Fig. 2b&c). (2) A constant bias square pulse to record t-on (Fig.5a). (3) A constant bias immediately following the switching pulse to record the t-off (Fig.6a). (4) A two-pulse that sandwiches a relaxation period to compare the V_{th} before/after the relaxation (Fig.7a).

Area-independence of conduction/leakage current at on/off states: The leakage current (I_{leak}) at low bias in devices of various sizes is measured before/after the first fire (FF) (Fig.3). In a fresh device before the FF, I_{leak} is area-dependent, and it becomes area-independent after the FF. This indicates that a filament is formed/activated by the FF, which dominates the conduction even at the off state at low bias. The current at both on-/off-states in subsequent switching are area independent (Fig.4a&4b&Fig.3b), supporting that the filament is modulated by the electric field, and becomes more/less conductive at on/off states, respectively.

Weibull distribution of time-to -switch-on/off (t-on/t-off): It is well known that the time-dependent-breakdown (TDDB) is caused by random defect generation through the formation of a filamentary percolation conduction path, following a Weibull distribution [4]. t-on in $\text{Ge}_x\text{Se}_{1-x}$ OTS follows a Weibull distribution during a constant stress with a bias lower than V_{th} (Fig. 5a&b). t-on (t_{63}) reduces exponentially with higher bias (Fig.5c), also in agreement with TDDB theory. t-off also follows Weibull distribution (Fig.6a&b). t-off increases exponentially with bias (Fig. 6c), opposite to t-on (Fig.5c). This suggests that the switch-off is the opposite

process to the switch-on, both governed by the same mechanism, most likely associated with defect discharging/charging, respectively. Switching-on/off in OTS modulates the filamentary percolation path following Weibull distribution, but the switching mechanism in OTS is fundamentally different from TDDB, as further investigated below.

Relaxation and the mechanism: To provide further support to the switching mechanism in OTS, it is observed in Fig. 7a&b that two consecutive switching in OTS can lead to a V_{th} reduction in the 2nd switching after a short relaxation. The value of $V_{th2}-V_{th1}$ (or $(V_{th2}-V_{th1})/V_{th1}$) is dependent on the relaxation conditions, reduced at longer relaxation times (t_{relax}), and V_{th2} can even exceed V_{th1} without signs of saturation at 1000 s (Fig. 8a-c). The median value of $(V_{th2}-V_{th1})/V_{th1}$ changes linearly against $\log(t_{relax})$ (Fig. 8c). V_{th2} recovery is accelerated at higher T_{relax} and V_{relax} , and is independent of device sizes (Fig.9a-c). Ge-rich ($x=60\%$) OTS recovers faster than Se-rich($x=40\%$) (Fig.10). This V_{th} reduction and recovery is clearly different from the defect generation in TDDB or defect migration during the switching in RRAM. It is further supported by RTN signals, which are caused by defect charging/discharging, observed during the relaxation (Fig.11), confirming that the filamentary conduction path can be blocked by trapping partially or fully (causing on/off oscillation).

Simulation: Theoretical simulation confirms the above experimental results. Mobility gap states are originated from Ge-Ge bonds, activated by FF, and form a chain of step-stones in OTS (Fig.12a&b), where Ge-Ge chains form delocalized/localized states, leading to on/off states, respectively. Ge-Ge bonds become localized gradually during relaxation (Fig.12c), leading to the V_{th2} reduction at short relaxation time, and its gradual recovery which is accelerated at higher temperatures.

Discussions: All the above results support that the switching on/off in OTS are associated with the delocalization/localization of defects. FF creates a filamentary percolation path formed by activated defects (Fig.3b). At high fields, these defects are delocalized in space and electrically charged/neutralized (depending on electron/hole trapping/de-trapping; electron is used as example in the following) [2], so that the filament can conduct a large current (Fig.4). At lower fields, this process is reversed and the filament becomes weaker (Fig.3). Immediately after the switch-off, some defects remain delocalized, leading to reduced V_{th} in the subsequent switching (Fig.7). The localization of these defects results in the slow V_{th} recovery, accelerated at higher temperature (Figs.9a&12c) and higher bias (Fig.9b). An illustration of the possible correlation between de/localization and discharging is shown in Fig.12d. Weibull distribution and the kinetics of t-on/-off against the bias also support this correlation, as charging and discharging have opposite bias dependence (Figs.5c&6c). Further defect localization at longer relaxation time and higher relaxation bias and temperature can even lead to V_{th2} larger than V_{th1} (Fig.8c&9a&9b), due to the de/localization balance during the V_{th} measurement.

Conclusions: Experimental and theoretical evidence is provided in this work to support filamentary-type switching in $\text{Ge}_x\text{Se}_{1-x}$ OTS selector. Conduction currents at on/off states are both area independent, and time-to-switch-on/-off follows Weibull distribution. V_{th} relaxation is observed and associated with defect delocalization/localization. The dependence of the switching and relaxation/recovery on bias/temperature are investigated and in good agreement with theoretical simulation results, providing new insights to the OTS switching and relaxation mechanism.

Reference: [1] [1] B. Govoreanu, et al, VLSI Symposium Tech. 2017. [2] S. Clima, et al, IEDM 2017. [3] N. S. Avasarala et al, VLSI Symposium Tech. 2018. [4] E. Wu, et al, IEDM 2017. [5] Z. Chai, et al, VLSI, 2016. [6] J. Ma, et al, IEDM, 2016.
Acknowledgement: EPSRC of UK (Grant nos.: EP/M006727/1 & EP/S000259/1).

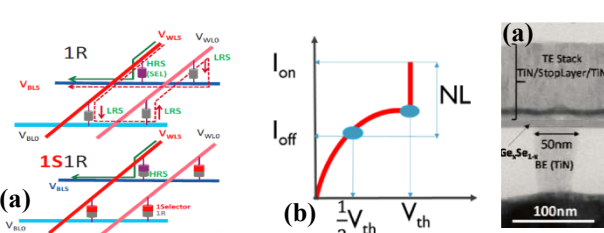


Fig.1 (a) High-performance selector devices are critical for high-density cross-point memory arrays (b) high half-bias nonlinearity is required to suppress sneak path current.

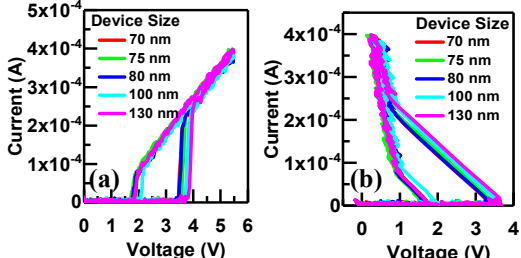


Fig.4 Volatile switching I-V curves of (a) 1S1R ($R=13\text{ k}\Omega$) and (b) 1S (same data as in (a), $V_{IS}=V_{ISIR}-V_{IR}$, shows area-independence at on-state).

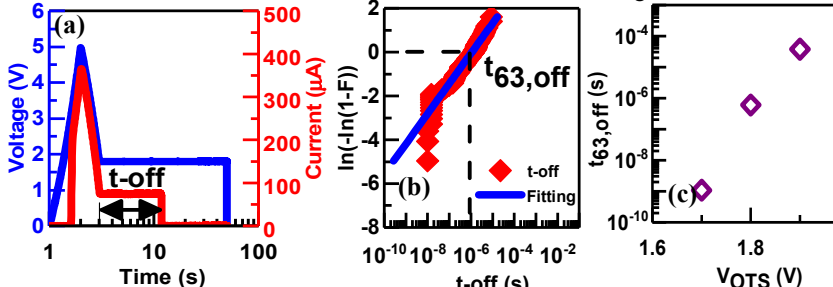


Fig.5 (a) Typical waveform (2.6V) for measuring t-on; (b) t-on follows Weibull distribution fitting ($V=2.6\text{ V}$). Test data at both ends are beyond measurement limitation. (c) t_{63} value of t-on decreases against bias.

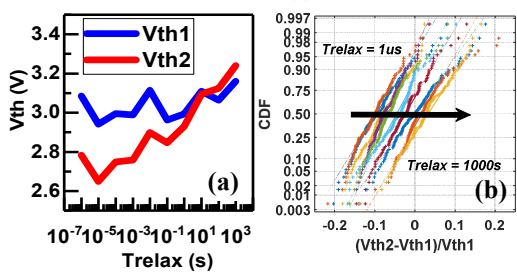


Fig.8 (a) V_{th1} and V_{th2} vs relaxation time. (b) $(V_{th2}-V_{th1})/V_{th1}$ distribution shifts with the relaxation time (c) the median value of $(V_{th2}-V_{th1})/V_{th1}$ changes linearly against $\log(t_{relax})$. Time interval between tests is 10 s to allow V_{th1} to recover.

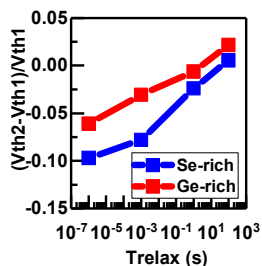


Fig.10 Ge-rich ($x=60\%$) OTS device recovers faster than the Se-rich ($x=40\%$) device. Relative recovery is used because of different V_{th} in two materials.

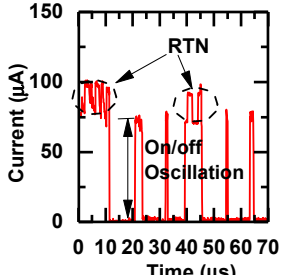


Fig.11 RTN signals and on/off oscillations are observed. On/off oscillations appears only when V_{relax} is low ($V_{relax}=2\text{ V}$).

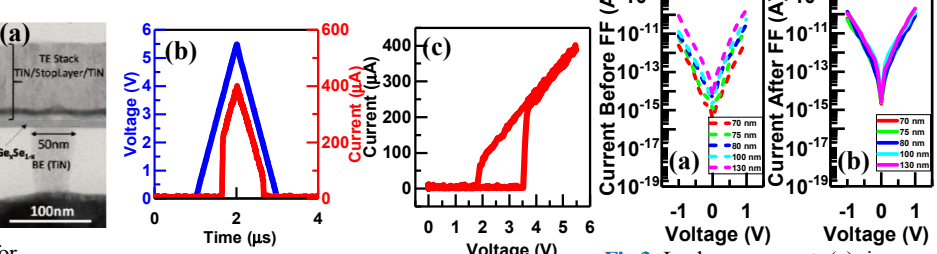


Fig.2 (a) OTS structure (in series with a $13\text{k}\Omega$ resistor). (b) Triangle voltage pulse and I-t. (c) I-V of volatile switching.

Fig.3 Leakage current (a) is area dependent at fresh-state before FF. (b) is area independent after FF.

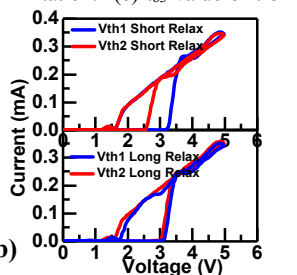
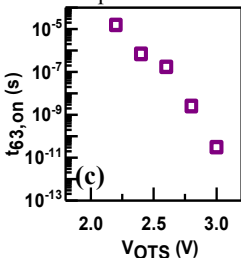


Fig.7 (a) V-t and I-t of two consecutive switching pulses sandwiching a relaxation period. (b) Short relaxation (1 μs) leads to a reduction in V_{th2} , which can recover at longer relaxation times (1 sec).

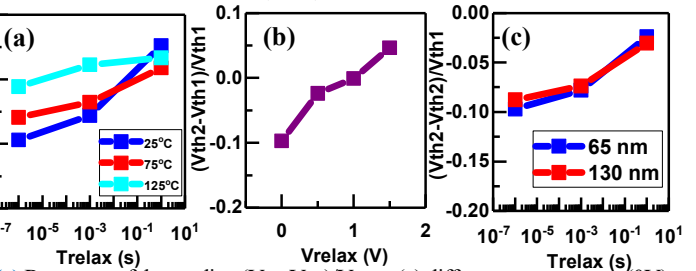


Fig.9 (a) Recovery of the median $(V_{th2}-V_{th1})/V_{th1}$ at (a) different temperatures (0V) and (b) different bias (25°C , 1s). Higher temperature and bias accelerate the recovery. (c) Negligible difference in V_{th} recovery in devices with different sizes confirms filamentary switching.

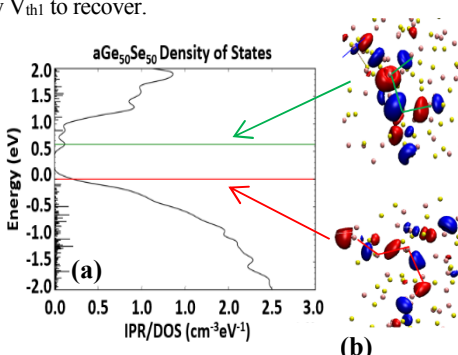


Fig.12 (a) Theoretical simulation of mobility gap states formed by Ge-Ge bonds and (b) Examples of Ge-Ge chain at conduction/valence band edges as electron/hole traps. (c) Relaxation of delocalized Ge-Ge bonds with time and temperature. (d) Illustration of the possible correlation between the defect's (1) charging (2) delocalization (3) discharging and (4) localization process (electron trapping/de-trapping as example).